SOME EPIDEMIOLOGICAL MODELS WITH NONLINEAR INCIDENCE

H.W. HETHCOTE AND P. VAN DEN DRIESSCHE

DMS–528–IR

December 1989
[Revised July 1990]

July 4, 1990

Some epidemiological models with nonlinear incidence

H.W. Hethcote[1] * and P. van den Driessche[2] **

[1]Department of Mathematics, University of Iowa, Iowa City, IA 52242, U.S.A.
[2]Department of Mathematics and Statistics, University of Victoria, Victoria, B.C. V8W 3P4, Canada

* Research supported in part by Centers for Disease Control Contract 200–87–0515. Support services provided at University House Research Center at the University of Iowa.

** Research supported in part by NSERC A–8965 and the University of Victoria President's Committee on Faculty Research and Travel.

Abstract. Epidemiological models with nonlinear incidence rates can have very different dynamic behaviors than those with the usual bilinear incidence rate. The first model considered here includes vital dynamics and a disease process where susceptibles become exposed, then infectious, then removed with temporary immunity and then susceptible again. When the equilibria and stability are investigated, it is found that multiple equilibria exist for some parameter values and periodic solutions can arise by Hopf bifurcation from the larger endemic equilibrium. Many results analogous to those in the first model are obtained for the second model which has a delay in the removed class but no exposed class.

Key words: Epidemiological model — Nonlinear incidence — Hopf bifurcation — Time delay

1. Introduction

Although the incidence rate (the rate of new infections) in most epidemiological models is bilinear in the infectious fraction I and the susceptible fraction S, actual incidence rates are probably not strictly linear in each variable over the entire range of I and S. For example, a less than linear response in I could occur due to saturation, where the infectious fraction is high so that exposure is very likely. The response could be greater than linear if the infectious fraction were very small or if multiple exposures were necessary for infection. These conceptual deviations from bilinear incidence would be difficult to verify through measurements of incidence rates or dynamical behavior. In general, data on infectious disease transmission is limited by measurement errors, asymptomatic cases, underreporting, stochastic environmental effects, expense, ethical considerations and other data collection difficulties. Although it is unlikely that nonlinear incidence could be verified or refuted using data, the conceptual possibilities make it imperative to investigate its effects on epidemiological models. The usefulness of epidemiological modeling concepts and applications depend on understanding the effects of changes in formulations on the behavior of solutions of the models.

Previous investigators cited below have shown that the qualitative dynamical behavior of epidemiological models with nonlinear incidence can be different from that of models with bilinear incidence. The latter exhibit the usual pattern in which the disease dies out (below the threshold) or approaches an equilibrium (above the threshold). Periodic solutions have been found for models with nonlinear incidence, even without periodic forcing. Here we investigate the effects of more general forms of nonlinear incidence on the dynamical behavior of two epidemiological models.

In these models a constant population is divided into disjoint classes based on disease status. At time t, let S(t) be the fraction of the population which is susceptible, E(t) be the fraction which is exposed but not yet infectious, I(t) be the infectious fraction, and

R(t) be the fraction which is removed with immunity. The first model considered is called an SEIRS model since susceptibles become exposed, then infectious, then removed and then susceptible again after the temporary immunity is lost. The vital dynamics are modeled by equal birth and death rates so that the total population is constant with all newborns entering the susceptible class. This model (Part I) consists of a system of nonlinear ordinary differential equations with a general nonlinear incidence rate $\beta g(I)S$ instead of the usual bilinear incidence rate βIS. If the exposed period is relatively short, then it can be eliminated so that susceptibles move directly to the infectious class. The second model (Part II) is an SIRS model with vital dynamics and a delay in the removed class corresponding to a constant period of temporary immunity. These models are analysed together in this paper since the equilibria and stability results are quite similar.

Nonlinear incidence rates of the form $\beta I^p S^q$ in ordinary differential equation SEIRS models with vital dynamics were investigated by Liu *et al.* (1986, 1987). They found that the dynamical behavior is not qualitatively altered by changing q from one, but it is altered significantly by changing p from one. For $p > 1$ they found multiple equilibria for some parameter values and periodic solutions arising by Hopf bifurcation for certain parameter values. More general forms of nonlinear incidence are considered in the first model here in order to better understand which forms of nonlinear incidence rates can lead to periodic solutions.

Models of SIR, SIRS and SEIS types with bilinear incidence and time delays were considered by Hethcote and Tudor (1980), Hethcote *et al.* (1981a, 1981b) and van den Driessche (1983). They found that sufficiently long time delays corresponding to temporary immunity in SIRS models can lead to periodic solutions. Since nonlinear incidence and time delays in the removed class can each lead to periodic solutions, Hethcote *et al.* (1989) investigated an SIRS model with both nonlinear incidence $\beta I^p S$ and a time delay in the removed class (but without vital dynamics) in order to explore possible synergistic effects on the periodic solutions. This work is extended here by considering an

SIRS model with a general nonlinear incidence rate $\beta g(I)S$, a time delay in the removed class and vital dynamics. Again the goal is to investigate which forms of nonlinear incidence can yield periodic solutions.

The effects of the formulation of epidemiological models on the global dynamical behavior of the solutions is important to epidemiological modellers. They must know whether the disease free equilibrium is stable or unstable, whether there are multiple endemic equilibria, whether these endemic equilibria are stable or unstable, what the basins of attraction are for the equilibria, and whether or not there are periodic solutions. A survey of mathematical disease transmission models was given by Hethcote *et al.* (1981c); a more recent survey of model formulations which lead to periodic solutions is in Hethcote and Levin (1989).

Part I: SEIRS Model with Vital Dynamics

2. SEIRS model formulation

In the transfer diagram

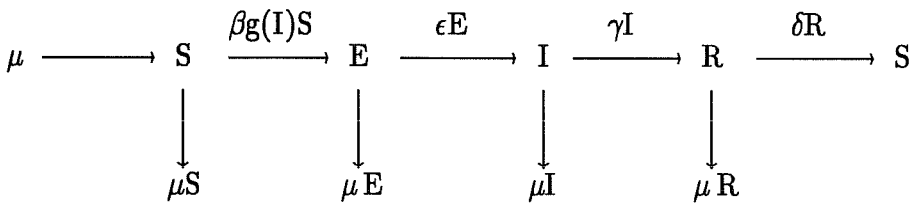

S, E, I, R denote respectively the fractions of the population that are susceptible, exposed (not yet infectious), infectious and recovered with temporary immunity. The parameter $\delta \geq 0$ is the rate constant for loss of immunity, γ is the rate constant for recovery, ϵ is the rate constant for the exposed population becoming infectious and $\mu \geq 0$ is the birth (and death) rate constant with all newborns assumed to be susceptible; β, γ, ϵ, $\delta + \mu$ are positive constants. The nonlinear incidence is assumed to be of the form $\beta g(I)S$, so the force of infection is $\beta g(I)$, where $g(0) = 0$, $g(I) > 0$ for $I \in (0,1]$ and $g \in C^3(0,1]$. The classical bilinear incidence (mass action) has $g(I) \equiv I$, and β is then the constant contact rate. The total population is assumed to be constant and the four classes to be disjoint, so that, for all time t,

$$S(t) + E(t) + I(t) + R(t) = 1. \tag{2.1}$$

The differential equations for the model can be written as

$$\begin{aligned} E' &= \beta g(I)(1-E-I-R) - (\epsilon+\mu)E, \\ I' &= \epsilon E - (\gamma+\mu)I, \\ R' &= \gamma I - (\delta+\mu)R. \end{aligned} \tag{2.2}$$

Note that (2.1) has been used to substitute for S in the first of these equations. The fraction initially infective is given by $I_0 = I(0) \geq 0$, and similarly for the other fractions.

By examining (2.2) on each boundary surface, we can show (as in Hethcote, 1978) that the region

$$B = \{(E,I,R) : E \geq 0, I \geq 0, R \geq 0, E + I + R \leq 1\} \tag{2.3}$$

is positively invariant with respect to the model. The continuity of the right side of (2.2) implies that solutions exist in B and since solutions remain in B, they are continuable for all $t \geq 0$ (see Hale, 1969, p. 14–17). If $g \in C^1[0,1]$, then the right side of (2.2) is globally Lipschitzian in B so that the initial value problem has a unique solution for all $t \geq 0$ which depends continuously on the data. If $g'(0)$ is unbounded, such as for $g(I) = I^p$ with $p < 1$, then $g'(I)$ is still bounded on $[\epsilon,1]$. In the domain D which is the interior of B, the right side of (2.2) is locally Lipschitzian since a Lipschitz constant exists for every closed bounded subset of D. Thus for any point in D, the initial value problem has a unique solution for all $t \geq 0$ which depends continuously on the data and parameters (Hale, 1969, p. 18–27). Solutions in B starting on the R axis approach the origin, but for all other starting points on the boundary of B, the solutions enter the interior of B so the initial value problem is well posed in the closed set B.

3. Equilibrium states for SEIRS model

The system of equations always has the trivial, disease free equilibrium (DFE), namely $(E,I,R) = (0,0,0)$ and $S = 1$. Also there may exist nontrivial endemic equilibria (E_e,I_e,R_e) where I_e satisfies the equation

$$\frac{1}{\sigma} = \frac{g(I)}{I}\left[1 - \frac{I}{H}\right] \equiv f(I), \tag{3.1}$$

and $$E_e = \frac{\gamma + \mu}{\epsilon} I_e, \quad R_e = \frac{\gamma}{\delta + \mu} I_e, \text{ and } S_e = 1 - \frac{I_e}{H},$$

where $$H \equiv \frac{\epsilon(\delta+\mu)}{\gamma\epsilon + (\delta+\mu)(\epsilon+\gamma+\mu)} < 1, \quad \sigma \equiv \frac{\beta\epsilon}{(\epsilon+\mu)(\gamma+\mu)}, \tag{3.2}$$

as in Liu *et al.* (1987). Here H is the maximum possible value of I_e, and, in the classical mass action case, σ is called the contact (reproduction) number.

The number of solutions of (3.1) depends on the nonlinear incidence function, and in particular on $\lim_{I \to 0} g(I)/I \equiv f(0)$ and the sign of $f'(I)$. Note that $f(I)$ is positive for $I \in (0,H)$ and $f(H) = 0$. Assume that $g(I)$ is such that either $f(0) > 0$ and $f(I)$ is monotonically decreasing ($f'(I) < 0$ on $(0,H]$), or $f(0) = 0$ and $f(I)$ is a unimodal function ($f''(I) < 0$ on $(0,H]$) with a unique interior maximum at $I = I_m$ and no other critical points. In the latter case the interior maximum occurs when

$$\frac{g'(I)}{I}\left[1 - \frac{I}{H}\right] = \frac{g(I)}{I^2}. \tag{3.3}$$

At $I = I_m$, the unique value of σ satisfying (3.1) is denoted by σ^*. These two equations give

$$\frac{1}{\sigma^*} = f(I_m) = \frac{g^2(I_m)}{I_m^2 \; g'(I_m)}, \tag{3.4}$$

and $$S_m = g(I_m)/(I_m\, g'(I_m)).$$

The equilibrium results are now summarized using the notation defined above.

Theorem 3.1. *The system* (2.2) *always has the disease free equilibrium* (0,0,0), *and if*

(i) $f(0) \leq 1/\sigma$ *and* $f'(I) < 0$ *for all* $I \in (0,H)$, *then it has no nontrivial equilibrium,*

(ii) $f(0) > 1/\sigma$ *and* $f'(I) < 0$ *for all* $I \in (0,H)$, *then it has* 1 *nontrivial equilibrium,*

(iii) $f(0) = 0$, $f''(I) < 0$ on $(0,H]$ *and* $\sigma < \sigma^*$, *then it has no nontrivial equilibrium,*

(iv) $f(0) = 0$, $f''(I) < 0$ on $(0,H]$ *and* $\sigma = \sigma^*$, *then it has* 1 *nontrivial equilibrium,*

(v) $f(0) = 0$, $f''(I) < 0$ on $(0,H]$ *and* $\sigma > \sigma^*$, *then it has* 2 *nontrivial equilibria* I_1, I_2 *where* $0 < I_1 < I_m < I_2 < H$.

In order to proceed further, we consider the nonlinear incidence function given by

$$g(I) = I^p/(1+\alpha I^q) \tag{3.5}$$

with parameters $p,q, > 0$, $\alpha \geq 0$. This generalizes the classical mass action incidence ($p = 1$, $\alpha = 0$), the nonlinear incidence I^p used by Liu *et al.* (1986, 1987) and Hethcote *et al.* (1989) ($\alpha = 0$), a more general incidence used by Liu *et al.* (1986) ($q = p - 1$) and saturated mass action used by Capasso and Serio (1978), Hethcote *et al.* (1981b), and Busenberg and Cooke (1988) ($p = q = 1$). Note that this latter case has the same form as a type II functional response introduced for biological interaction models by Holling (1959). For the function (3.5), equation (3.3) becomes

$$(p + \alpha(p-q)I^q)(1 - I/H) = 1 + \alpha I^q, \tag{3.6}$$

which is an implicit equation for I_m. From (3.4) the value σ^* of σ at $I = I_m$ satisfies

$$\frac{1}{\sigma^*} = \frac{I_m^{p-1}}{p + \alpha(p-q)I_m^q} \quad . \tag{3.7}$$

Two important cases of (3.5) are (3.5a) $q = p$ and (3.5b) $q = p - 1$. In both these cases, when $p > 1$, there is a unique I_m and σ^* given by (3.6) and (3.7) respectively. The number of nontrivial equilibria for these cases, interpreted from Theorem 3.1, is summarized in Table 1. Note that, for the special case (3.5a) with $p = q = 1$, the classical threshold $\sigma = 1$ (independent of α) is retained. For the special case (3.5b) with $q = p - 1$, when $p < 1$ the threshold is $\sigma = \alpha$. Whereas in this case when $p = 1$, then $\sigma = 1 + \alpha$ is the threshold value, so there is no nontrivial equilibrium if $\sigma \leq 1 + \alpha$ and there is one nontrivial equilibrium if $\sigma > 1 + \alpha$. For $g(I) = I^p$ (that is (3.5) with $\alpha = 0$), Figure 1 of Liu *et al.* (1987) provides a generic illustration of how the number of equilibria is determined.

4. Stability of the disease free equilibrium for SEIRS model

To examine the local stability of the disease free equilibrium (DFE) which has $E = I = R = 0$ (and so $S = 1$), we linearise the system (2.2) about this point, giving the Jacobian matrix

$$J_0 = \begin{bmatrix} -(\epsilon+\mu) & \beta g'(0) & 0 \\ \epsilon & -(\gamma+\mu) & 0 \\ 0 & \gamma & -(\delta+\mu) \end{bmatrix}.$$

As $\delta + \mu > 0$, the eigenvalues of J_0 have negative real parts so that the DFE is locally asymptotically stable (LAS) iff

$$1/\sigma > g'(0) = f(0). \tag{4.1}$$

For model (3.5a), when $p < 1$, the DFE is unstable. When $p = 1$ (mass action), the DFE is LAS if $\sigma < 1$ and unstable when $\sigma > 1$. When $p > 1$ the DFE is always LAS. For model (3.5b), when $p < 1$, the DFE is LAS if $\sigma < \alpha$, and unstable if $\sigma > \alpha$. When $p = 1$ (mass action with contact rate $\beta/(1+\alpha)$), the DFE is LAS if $\sigma < 1 + \alpha$ and unstable if $\sigma > 1 + \alpha$. When $p > 1$, the DFE is always LAS, as found in the corresponding SIRS model by Liu *et al.* (1986, Section 5).

With some restrictions on the incidence, we can use a Lyapunov function (as in Liu *et al.* (1987, Section 3)) to give a global stability result for a restricted set of σ values.

Theorem 4.1. *Assume that* $g \in C^1[0,1]$, σ^* *exists and* $1/\sigma_1 \equiv \max\{g(I)(1-I)/I\}$ *for* $I \in [0,1]$ *is finite. Then for* $\sigma < \sigma_1$, *all solutions of the model* (2.2) *which start in the feasible region* B *given by* (2.3) *approach the disease free equilibrium as* $t \to \infty$.

Proof. Consider the Lyapunov function

$$L = E + \frac{(\epsilon+\mu)I}{\epsilon},$$

then from (2.2)

$$L' = \frac{\beta}{\sigma} I\left[-1 + \sigma \frac{g(I)}{I}(1-I-E-R)\right]$$

$$\leq \frac{\beta}{\sigma} I\left[-1 + \sigma \frac{g(I)}{I}(1-I)\right]$$

$$\leq \frac{\beta}{\sigma} I\left[-1 + \frac{\sigma}{\sigma_1}\right].$$

So for $\sigma < \sigma_1$, $L' \leq 0$. Since $\sigma < \sigma_1 < \sigma^*$, equality for $L' = 0$ holds only when $I = 0$. Thus $E = I = R = 0$ is the largest invariant subset in the set where $L' = 0$. So by a LaSalle extension of the Lyapunov theorem (see *e.g.* Miller and Michel (1982, p. 227)), the result is proved. ∎

This theorem shows that with the incidence function $g(I)$ given by (3.5), for $p > 1$, the DFE is globally asymptotically stable (GAS) for $\sigma < \sigma_1 \leq p^p/(p-1)^{p-1}$. We conjecture this global stability actually holds for $\sigma < \sigma^*$.

For $p = 1$, the same Lyapunov function shows that the DFE is GAS for σ values below and on the threshold given in Section 3. The classical threshold behaviour is thus retained when $p = 1$, with the threshold at $\sigma = 1$ in model (3.5a) but at $\sigma = 1 + \alpha$ in model (3.5b). But for $p > 1$ the asymptotic behaviour is less clear as it depends on σ^* and on the initial values.

For $p < 1$ in model (3.5a) the threshold is lost. In this case, in the feasible region near the origin, S is bounded away from zero because, when $S = 0$, $S' = \mu + \delta R$. There exists a value of I sufficiently small so that $L' > 0$ and so all solutions (except those starting on the R axis) move away from the origin. For $p < 1$ in model (3.5b), the same

Lyapunov function shows that the DFE is GAS when $\sigma < \alpha$. Thus the primary difference between cases (3.5a) and (3.5b) occurs for $p < 1$ where the usual threshold result holds for case (3.5b), but there is no threshold for case (3.5a). Stability results for the DFE with g(I) given by (3.5) are summarized in Table 2.

5. Stability of endemic equilibria for SEIRS model

The local stability of an endemic equilibrium can be examined by linearizing system (2.2) about I_e. This gives the Jacobian matrix

$$J_e = \begin{bmatrix} -(\beta g(I_e) + \epsilon + \mu) & \beta(S_e\, g'(I_e) - g(I_e)) & -\beta g(I_e) \\ \epsilon & -(\gamma+\mu) & 0 \\ 0 & \gamma & -(\delta+\mu) \end{bmatrix}$$

where $S_e = 1 - I_e/H$. Eigenvalues of J_e are solutions of the cubic equation

$$\lambda^3 + c_1\lambda^2 + c_2\lambda + c_3 = 0,$$

with
$$\left.\begin{aligned} c_1 &\equiv -\text{trace } J_e > 0, \\ c_2 &\equiv M \equiv \Sigma(2 \times 2 \text{ principal minors of } J_e), \\ c_3 &\equiv -\det J_e = -(\epsilon+\mu)(\delta+\mu)(\gamma+\mu)(K-y-1), \end{aligned}\right\} \tag{5.1}$$

where
$$K \equiv I_e\, g'(I_e)/g(I_e) \text{ and } y \equiv I_e/(H-I_e) > 0. \tag{5.2}$$

As trace $J_e < 0$, necessary and sufficient conditions for J_e to have all eigenvalues with negative real parts are $\det J_e < 0$ and $C \equiv M(\text{trace } J_e) - \det J_e < 0$. Taking $b = \beta/\sigma$, so $b\,Hy = \beta g(I_e)$ from (3.1), gives

$$M \equiv (\epsilon+\gamma+\delta+2\mu)\, bHy + (\delta+\mu)(\epsilon+\gamma+2\mu) - (\epsilon+\mu)(\gamma+\mu)(K-1). \tag{5.3}$$

We proceed as in Liu *et al.* (1987, Section 5) by writing

$$C \equiv C(y) = a_2(bHy)^2 + a_1(bHy) + a_0, \tag{5.4}$$

where $a_2 \equiv -(\epsilon+\gamma+\delta+2\mu) < 0, \quad a_1 \equiv (\epsilon+\mu)(\gamma+\mu)(K-1) - B,$

$$a_0 \equiv (\epsilon+\gamma+2\mu)(\epsilon+\mu)(\gamma+\mu)(K-1) - (\delta+\mu)(\epsilon+\gamma+2\mu)(\epsilon+\gamma+\delta+3\mu),$$

and $$B \equiv (\epsilon+\gamma+\delta+3\mu)^2 - (\epsilon+\mu)(\gamma+\mu) - \mu^2 > 0.$$

Note that the coefficients a_1 and a_0 depend (in general) on y. However, in the case $g(I) = I^p$, as considered by Liu *et al.* (1987), $K = p$, a constant, and so (5.4) is a quadratic in y.

When $I_e g'(I_e) \leq g(I_e)$, then $K \leq 1$, giving $\det J_e < 0$ and $C < 0$, so the equilibrium is locally asymptotically stable (LAS). For $g(I)$ such that I_m exists, then at $I = I_m$, $\sigma = \sigma^*$, and $K - 1 - y = 0$. Also for $I = I_1 < I_m$, $\sigma > \sigma^*$ and $K - 1 - y > 0$. Thus (5.1) shows that $\det J_e > 0$ at the smaller endemic equilibrium, I_1, so that this equilibrium is unstable. At the larger endemic equilibrium, $I_2 > I_m$, $K - 1 - y < 0$ so $\det J_e < 0$; thus the stability of I_2 depends on the sign of C. When $C < 0$, the larger endemic equilibrium I_2 is LAS; when $C > 0$, it is unstable. When $C = 0$, there is a negative real eigenvalue and a pair of purely imaginary eigenvalues $\lambda = \pm i\sqrt{M}$. If such a purely imaginary eigenvalue exists, then it is a simple eigenvalue, and no integral multiple is an eigenvalue. Thus for suitable parameter values a Hopf bifurcation can occur for a particular value of $\sigma > \sigma^*$ so that there is a periodic solution around the larger endemic equilibrium.

With $g(I)$ given by (3.5),

$$K = \frac{p + \alpha(p-q)I_e^q}{1 + \alpha I_e^q}. \tag{5.5}$$

So, if $p \leq 1$, $p + \alpha(p-q)I_e^q \leq 1 + \alpha I_e^q$, giving $K \leq 1$ (independent of q). Thus in system (2.2) if $g(I) = I^p/(1+\alpha I^q)$ and exactly one nontrivial equilibrium exists according to the results in Section 3, then for $p \leq 1$, this equilibrium is LAS.

Now consider the possibilities with this $g(I)$ for $p > 1$. When $\sigma < \sigma^*$, there is no nontrivial equilibrium and when $\sigma = \sigma^*$ there is a saddle–node bifurcation. When $\sigma > \sigma^*$ (so that there are two endemic equilibria), it has been shown above that the smaller equilibrium is unstable, and the behaviour at the larger equilibrium depends on the sign of C. More details on this are given in the following section.

6. Hopf bifurcation

Throughout this section we consider $g(I)$ given by (3.5) and the larger equilibrium $I_2 \in (I_m,H)$. Equation (5.2) gives $y_m < y < \infty$ on this interval, where

$$y_m = I_m/(H-I_m). \tag{6.1}$$

Also $K = y + 1$ at $I = I_m$, and

$$K_m = y_m + 1, \tag{6.2}$$

is the maximum value of K on this interval. Because the coefficients of $C(y)$ in (5.4) are analogous to those in Liu *et al.* (1987, Section 5), the analysis there implies that if

$$(\delta+\mu)^2 < \gamma\epsilon \tag{6.3}$$

and

$$K_m > K_1 \equiv 1 + \frac{(\delta+\mu)(\epsilon+\gamma+2\mu)\ [\gamma\epsilon + (\delta+\mu)(\epsilon+\gamma+\mu)]}{(\epsilon+\mu)(\gamma+\mu)\ [\gamma\epsilon - (\delta+\mu)^2]}, \tag{6.4}$$

then we can iteratively solve $C = 0$ for the root $I_2 \in (I_m,H)$, and from (3.1) compute the Hopf bifurcation value of σ as

$$\sigma^{**} = \frac{1 + \alpha I_2^q}{I_2^{p-1}(1-I_2/H)}. \tag{6.5}$$

Condition (6.3) would usually be satisfied since the death–adjusted average period of temporary immunity $1/(\delta+\mu)$ would usually be greater than both the average latent

period $1/\epsilon$ and the average infectious period $1/\gamma$. For models (3.5a) and (3.5b), $K_m > K_1$ in condition (6.4) iff $p > p_1 > K_1$ where p_1 must be found iteratively. We have shown above that if condition (6.3) and (6.4) are satisfied, then Hopf bifurcation occurs at $\sigma = \sigma^{**} > \sigma^*$. When $\sigma > \sigma^{**}$, then $C(y_2) < 0$ so that the larger endemic equilibrium is LAS. When $\sigma^{**} > \sigma > \sigma^*$, then $C(y_2) > 0$ so that it is unstable. When one of the conditions (6.3) or (6.4) is not satisfied, then $C(y_2) < 0$ so that the larger equilibrium is LAS.

The stability of the periodic solutions generated by Hopf bifurcation for the three dimensional system (2.2) and the direction of bifurcation depend on the sign of the value of a stability quantity A at the bifurcation point. This stability quantity A for our system is the same as in the model of Liu *et al.* (1987), except that their constant p is replaced by K. Their A was derived using the center manifold theorem, perturbation theory and the criterion for super– or sub–critical Hopf bifurcation in two dimensional space. For given parameter values the value of A is calculated numerically.

7. Hopf bifurcation numerical calculations

For nonlinear incidence with g(I) given by (3.5), a computer program has been used to calculate the quantities in sections 3, 5 and 6 when parameter values are input. First, I_m, σ^* (the saddle–node bifurcation value of σ), y_m and K_m are found by solving equation (3.6) using Newton's method and then using (3.7), (6.1) and (6.2). Next conditions (6.3) and (6.4) which are necessary for Hopf bifurcations are checked numerically. The lower bound p_1 of p for which Hopf bifurcation may occur can be found by bisection. Next, equation (5.4) is solved by the secant method for y_2. Then the larger endemic equilibrium $I_2 = Hy_2/(y_2+1)$ is used in (6.5) to calculate σ^{**} (the imaginary root surface) which gives the Hopf bifurcation value of σ.

For specific parameter values the projections from $p\alpha\sigma$ space onto the $p\alpha$ plane of the curves for $p = p_1$ where the Hopf bifurcation surface σ^{**} comes off the saddle node bifurcation surface σ^* are shown in Figure 1 for case (3.5a) $q = p$ and case (3.5b) $q = p-1$. In both cases p_1 is an increasing function of α. The parameter values are $\epsilon = 1$ (average latent period = 1 day), $\gamma = 0.0133$ (average infectious period = 75 days), $\delta = 0.0033$ (average immune period = 300 days) and $\mu = 0.00004$ (average lifespan = 68.5 years). For these parameter values and $\alpha = 0$, the value $p_1 = 1.32$, the saddle–node bifurcation curve σ^* and the Hopf bifurcation curve σ^{**} are shown in the $p\sigma$ plane in Figure 2 of Liu *et al.* (1987).

The transversality condition guarantees that the real part of the characteristic roots really does switch sign when σ crosses the imaginary root surface σ^{**}. We have found that at $\lambda = i\sqrt{M}$,

$$2(c_1^2+c_2)\,\lambda'(\sigma) = \frac{\partial c_3}{\partial \sigma} - c_2\frac{\partial c_1}{\partial \sigma} - c_1\frac{\partial c_2}{\partial \sigma} = \frac{\partial C}{\partial \sigma}, \qquad (7.1)$$

where $\lambda'(\sigma)$ is the real part of the derivative of λ with respect to σ. The value of (7.1) is calculated in the computer program in order to verify the transversality condition numerically. For some values of α, p and q, the transversality condition can be verified analytically. In all of our computer calculations the transversality condition is satisfied since $\lambda'(\sigma^{**})$ is negative. This means the real part of the complex pair changes from positive to negative as σ increases across the imaginary root surface σ^{**} so that the larger equilibrium is unstable for $\sigma < \sigma^{**}$ and is LAS for $\sigma > \sigma^{**}$.

As indicated in section 6, the sign of the stability quantity A determines the direction and stability of the Hopf bifurcation. In particular, when A is negative, there are stable periodic solutions around the unstable larger equilibrium for $\sigma < \sigma^{**}$; when A is positive, there are unstable periodic solutions around the LAS larger equilibrium for $\sigma > \sigma^{**}$. To compute A, we use the formulas of Liu *et al.*(1987, Appendix 1) noting that the constant p must be replaced by K from (5.5), since g(I) is given by (3.5). Since the Hopf bifurcation is generic, the radius of the periodic solution is proportional to $|\sigma - \sigma^{**}|^{\frac{1}{2}}$.

For specific parameter values the projections from $p\alpha\sigma$ space onto the $p\alpha$ plane of the curves for p_2 where the sign of the stability quantity A first switches from positive to negative are shown in Figure 1 for the cases $q = p$ and $q = p - 1$. In both cases p_2 is an increasing function of α. Thus the periodic solutions arising by Hopf bifurcation are unstable around the LAS larger endemic equilibrium with $\sigma > \sigma^{**}$ for $p_1 < p < p_2$ and are LAS around the unstable larger equilibrium with $\sigma < \sigma^{**}$ for some p values above p_2. For $\alpha = 0$, A is negative for $p_2 < p < p_3$ where $p_2 = 1.76$ and $p_3 \simeq 121$ and then A remains positive for $p > p_3$; the behavior is similar for $\alpha > 0$. For these specific parameter values and $\alpha = 0$, the value p_2 where the stability switches is shown in Figure 2 of Liu *et al.*(1987).

Part II: SIRS Model with Delay in R and Vital Dynamics

8. Model formulation

The transfer diagram below is similar to that in section 2, except that ω is the constant period of temporary immunity and the exposed class is not included as it has been found to have no qualitative effect on previous similar models.

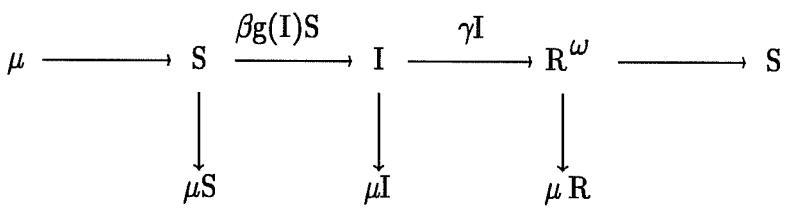

This model is an extension of the one considered in Hethcote *et al.* (1989) where $g(I)$ was I^p and vital dynamics was not included.

For all $t \geq 0$ the integral equation for $I(t)$ is

$$I(t) = I_0 e^{-(\gamma+\mu)t} + \beta \int_0^t g(I(y))S(y)e^{-(\gamma+\mu)(t-y)}\,dy, \tag{8.1}$$

where initially $I(0) = I_0$. The corresponding differential equation is

$$I'(t) = -(\gamma+\mu)I(t) + \beta g(I(t))S(t). \tag{8.2}$$

For the removed class, let $R_0(t)$ be the fraction initially removed and still removed at time t. Then

$$R(t) = \begin{cases} R_0(t)e^{-\mu t} + \gamma \int_0^t I(x)e^{-\mu(t-x)}\,dx, & \text{for } t \leq \omega, \\ \gamma \int_{t-\omega}^t I(x)e^{-\mu(t-x)}\,dx, & \text{for } t > \omega. \end{cases} \tag{8.3}$$

In this model, (2.1) is replaced by

$$S(t) + I(t) + R(t) = 1. \tag{8.4}$$

As in Hethcote *et al.* (1989), this model is well–posed and the positively invariant region is

$$B = \{(I,R) : I \geq 0,\ R \geq 0,\ I + R \leq 1\}. \tag{8.5}$$

9. Equilibrium states

This delay model always has the disease free equilibrium (DFE), namely (I,R) = (0,0) with S = 1. Nontrivial equilibria may exist where I_e satisfies (3.1) with

$$1/H = 1 + r, \quad r \equiv \gamma(1-e^{-\mu\omega})/\mu, \quad \sigma = \beta/(\gamma+\mu). \tag{9.1}$$

In the limit as $\mu \to 0$, $r \to \gamma\omega$ as in Hethcote *et al.* (1989) where vital dynamics is not considered. At such an equilibrium $R_e = rI_e$, and $S_e = 1 - (1+r)I_e$. With (9.1) the number of equilibria for the delay system is the same as that for (2.2) as summarized in Theorem 3.1. For the special case when g(I) is given by (3.5), the number of nontrivial equilibria is given in Table 1.

10. Stability of the disease free equilibrium

Local stability of the DFE is governed by (8.2) linearized about $I = 0$, namely

$$I'(t) = (\gamma+\mu)(-1 + \sigma g'(0))\, I(t). \tag{10.1}$$

Thus the DFE is LAS iff $1/\sigma > g'(0) = f(0)$. The local stability results are therefore independent of the delay, and are the same as those in Section 4.

Taking the Liapunov function $L = I$, the global stability result of Theorem 4.1 holds with the same value of σ_1, but the region B is given by (8.5). Stability results for the DFE with g(I) given by (3.5) are given in Table 2..

11. Stability of the endemic equilibria

Local stability of a nontrivial equilibrium I_e is governed by (8.2) linearized about this point. This gives the characteristic equation

$$\lambda + (\gamma+\mu) - \beta g'(I_e)S_e + \beta g(I_e)\left[1 + \frac{\gamma}{\lambda+\mu}(1 - e^{-\omega(\mu+\lambda)})\right] = 0. \qquad (11.1)$$

Letting $z = \omega\lambda$ and $s = \omega\mu > 0$, we obtain

$$\Delta(z) \equiv z + s + a + c(1-e^{-(z+s)})/(z+s) = 0 \qquad (11.2)$$

where

$$a \equiv \omega\gamma - \omega\beta\, g'(I_e)S_e + \omega\beta\, g(I_e) \qquad (11.3)$$

and

$$c \equiv \omega^2\beta\gamma\, g(I_e) > 0. \qquad (11.4)$$

Complex (including nonzero purely imaginary) roots of (11.2) occur in complex conjugate pairs. To locate the purely imaginary roots, set $z = iy$ $(y > 0)$ in (11.2) multiplied by $z + s$. Then equating real and imaginary parts gives

$$a = \frac{(y^2-s^2)e^{-s}\frac{\sin y}{y} + 2s(1-e^{-s}\cos y)}{se^{-s}\frac{\sin y}{y} - (1-e^{-s}\cos y)} \qquad (11.5)$$

$$c = \frac{-(y^2+s^2)}{se^{-s}\frac{\sin y}{y} - (1-e^{-s}\cos y)} \qquad (11.6)$$

as parametric equations for the imaginary root curve in the ac plane.

When $s = 0$, equation (11.2) reduces to the characteristic equation analysed in Hethcote *et al.* (1989); see also Hethcote *et al.* (1981b). Typically s is small; for example, if $\omega = 300$ days and $\mu = 0.00004$ as in Figure 1, then $s = \omega\mu = 0.012$. For small s and c the imaginary root curve given by (11.5), (11.6) and the zero root line are close to those in Figure 2 in Hethcote *et al.* (1989). For small, positive s and c the imaginary root curve is shifted left and the zero root line is moved left at the origin with a steeper negative slope. Results similar to those in Hethcote *et al.* (1989) are obtained below for the transcendental equation (11.2). This equation is also considered in Hao and Brauer (1990), where a graph of the imaginary root curve is given.

Theorem 11.1.

(*a*) *All roots of* (11.2) *with* $\operatorname{Re} z \geq 0$ *lie in a bounded domain.*

(*b*) *Equation* (11.2) *has a zero root iff* $s + a + c(1-e^{-s})/s = 0$.

(*c*) *If* $s + a + c(1-e^{-s})/s < 0$, *then* (11.2) *has at least one positive real root.*

(*d*) *If* $c < \{(a+s)^2 + s^2\}/2$, *then* (11.2) *has no* (*nonzero*) *purely imaginary roots.*

(*e*) *If* $s + a + c(1-e^{-s})/s > 0$, $a > 0$ *and* $c < \{(a+s)^2 + s^2\}/2$, *then all roots of* (11.2) *have negative real parts.*

(*f*) *If* $s + a + c(1-e^{-s})/s > 0$ *and* (a,c) *is below and to the right of the imaginary root curve given parametrically by* (11.5), (11.6), *then all roots have negative real parts.*

Proof.

(a) $|(z+s+a)(z+s)| = |c(1-e^{-(z+s)})| \leq 2c$.

(b) Setting $z = 0$ in (11.2) gives the stated equality.

(c) Since the left side of (11.2) is negative for $z = 0$ and approaches $+\infty$ as real z approaches $+\infty$, (11.2) must (by the intermediate value theorem) have a positive real root.

(d) Purely imaginary roots are given by setting $z = iy$ with $y > 0$. Rearranging and taking absolute values, we obtain

$$|(c-y^2+s^2+as) + iy(a+2s)| = |ce^{-s}(\cos y - i \sin y)|$$

so that $(c-y^2+s^2+as)^2 + (a+2s)^2y^2 \leq c^2$. Thus

$$0 < y^4 + 2c(s^2+a^2) + (s^2+as)^2 \leq y^2(2c-(a+s)^2-s^2),$$

implying that $0 < 2c - (a+s)^2 + s^2$.

(e) For $0 \leq \theta \leq 1$ consider

$$z + \theta s + a + c(1-e^{-(z+\theta s)})/(z+\theta s). \tag{11.7}$$

From Hethcote *et al.* (1989, Th. 5.1(d)), equation (11.7) has no roots with $\text{Re } z \geq 0$ for $\theta = 0$. Roots of (11.7) depend continuously on the parameter θ. As θ increases from 0, roots would have to enter the right half of the complex plane by coming in from infinity or crossing the imaginary axis. They cannot come from infinity by part (a). They cannot enter as (nonzero) purely imaginary roots by part (d). Since the hypotheses imply $\theta s + a + c(1-e^{-\theta s})/\theta s > 0$ for $a > 0$, they cannot enter as zero roots by part (b). Thus (11.7) has no roots with $\text{Re } z \geq 0$ for θ in $[0,1]$.

(f) The roots of (11.2) depend continuously on the coefficients a and c. As the region in part (e) is expanded to the region here, roots entering the right half of the complex plane would have to come in from infinity or cross the imaginary axis. They cannot enter from infinity by part (a) or as zero roots by part (b) or as (purely) imaginary roots since the first ones occur on the lower right boundary

given by (11.5), (11.6). Thus all roots have negative real parts. ∎

As in section 5 the smaller endemic equilibrium found from (3.1) is unstable.

Theorem 11.2. *For* $g(I)$ *such that* I_m *exists, and if* $f(0) = 0$ *and* $\sigma > \sigma^*$, *then the smaller endemic equilibrium* I_1 *in* $(0,I_m)$ *is unstable.*

Proof. From Theorem 3.1, two nontrivial equilibria exist in this case. Using the definitions of a and c above

$$s + a + c\left[\frac{1-e^{-s}}{s}\right] = (s+\omega\gamma)[1 + (1+r)\sigma g(I_1) - \sigma g'(I_1)S_1] \tag{11.8}$$

at the smaller equilibrium $I_1 < I_m$. At $I = I_m$ and $\sigma = \sigma^*$, we have $f'(I_m) = 0$ so that the expression in (11.8) is 0. For $I_1 < I_m$, $f'(I_1) > 0$ so $g'(I_1)S_1 > g(I_1)/I_1$ from which it follows that the above expression is negative. Part (b) of Theorem 11.1 implies that (11.2) has a positive real root so that I_1 is unstable. ∎

For the SIRS model considered here, we have obtained analytic results analogous to those in Part I and in Hethcote *et al.* (1989). We anticipate that the other results in Part I and in Hethcote *et al.* (1989) would also hold for this model. Specifically, the zero root curve given in Theorem 11.1 would lead to a saddle–node bifurcation surface $\sigma = \sigma^*$ and the lowest purely imaginary root curve given by (11.5), (11.6) would lead to a Hopf bifurcation surface $\sigma = \sigma^{**}$. We also anticipate that analogous stability results would hold for the larger endemic equilibrium I_2 and the Hopf–bifurcated periodic solutions. Since deviations from the pattern established seem unlikely, we have not carried out any further algebraic or numerical calculations for this model.

12. Discussion

In our analytical results and numerical calculations with different parameter values, we have found that the thresholds, the number of equilibria, their stability, the occurrence of Hopf bifurcation and the stability of the periodic solutions for the SEIRS model in Part I are qualitatively very similar when the nonlinear incidence is $\beta I^p S/(1+\alpha I^q)$ to those when it is $\beta I^p S$. These results also seem to carry over for the SIRS model with general nonlinear incidence and a delay considered in Part II. Thus the primary lesson of this paper is that general nonlinear incidence rates of the form $\beta g(I)S$ in epidemiological models do not lead to major changes in dynamical behavior when compared to that for nonlinear incidence of the form $\beta I^p S$.

For $g(I) = I^p/(1+\alpha I^q)$ with $\alpha > 0$ we found that the dynamical behavior differed in only one way from the $\alpha = 0$ behavior. Specifically, for $p < 1$ and $q = p - 1$ the usual epidemic threshold pattern holds for $\alpha > 0$ with the disease dying out below the threshold $(\sigma \leq \alpha)$ and the disease level approaching the endemic equilibrium above the threshold $(\sigma > \alpha)$. When $\alpha = 0$, there is no threshold so that the disease never dies out and always approaches the endemic equilibrium.

In the SEIRS model given by (2.2) with $g(I)$ given by (3.5), the choice of the value of p has a big impact on the dynamical behavior. For $p = 1$ the usual epidemiological pattern holds; namely, below the threshold the disease dies out and above the threshold the disease level approaches the unique endemic equilibrium. As seen in Tables 1 and 2, this usual epidemiological pattern holds for $p < 1$ and $q = p - 1$, but the threshold disappears completely when $p < 1$ and $q = p$ so that the disease never dies out and the disease level always approaches the unique endemic equilibrium.

In this SEIRS model with $p > 1$, the threshold concept becomes more complicated since the asymptotic behavior can depend on both the threshold and the initial conditions. Below the threshold $(\sigma < \sigma^*)$ the disease dies out; moreover, the disease also dies out

above the threshold for some initial conditions. Above the threshold ($\sigma > \sigma^*$) there are two endemic equilibria, but the smaller equilibrium is always an unstable saddle.

For this SEIRS model, periodic solutions appear through Hopf bifurcation at $\sigma = \sigma^{**}$ for $p > p_1$. When either $1 < p < p_1$ and $\sigma > \sigma^*$ or $p > p_1$ and $\sigma > \sigma^{**}$, the larger endemic equilibrium is locally attractive so that disease levels in some nearby region approach it. When $p > p_1$ and $\sigma^{**} > \sigma > \sigma^*$, the larger endemic equilibrium is repulsive. As shown in Liu *et al.* (1987), the stability quantity A is positive when $p \to p_1 + 0$ or when $p \to +\infty$ and ϵ stays bounded. Hence either A is always positive or A changes signs from positive to negative at p_2 and then changes back at p_3 (we cannot exclude multiple sign changes). Parameter sets illustrating the two possibilities are given in Liu *et al.* (1987). When A is positive, the repulsive periodic solution surrounds the attractive larger equilibrium with $\sigma > \sigma^{**}$. When A is negative, the attractive periodic solution surrounds the repulsive larger equilibrium with $\sigma < \sigma^{**}$. For g(I) given by (3.5) and parameter values corresponding to the second possibility above, there are also two sign changes for $\alpha > 0$ with the first sign change at p_2 shown in Figure 1 and the second sign change occurring at p_3, which is near the value of $p_3 = 121$ for $\alpha = 0$. In Hethcote *et al.* (1981a) there is a region in parameter space near the point on the Hopf bifurcation curve corresponding to the stability switch for the periodic solution where two periodic solutions (one stable and one unstable) exist simultaneously around the larger equilibrium. Since stability switches also occur along the Hopf bifurcation curve for the SEIRS model here, multiple periodic solutions could also exist here for parameter values near these switching points.

As described in Liu *et al.* (1987), the SEIRS model becomes an SIRS model when $\epsilon \to \infty$, an SEIS model when $\delta \to \infty$ and an SIS model when both ϵ and $\delta \to \infty$. Some global stability results are given there. Hopf bifurcation does not occur for the SIS and SEIS models. Phase plane plots are given for the SIRS model in Liu *et al.* (1986). These plots show features such as saddles, stable and unstable nodes, stable and unstable limit cycles,

show features such as saddles, stable and unstable nodes, stable and unstable limit cycles, homoclinic orbits and basins of attraction. The global behavior and bifurcation diagrams for the SIRS model are given in Liu *et al.* (1987).

The SIRS model given in Part II has a general nonlinear incidence rate and a delay in the removed class. The basic results for this model are included in this paper, since they are very similar to those for the models in Part I and in Hethcote *et al.* (1989). The detailed algebraic and numerical calculations related to Hopf bifurcation have not been carried out for this model, but we expect them to be similar to those for the same model with a less general nonlinear incidence rate in Hethcote *et al.* (1989).

In this paper the epidemiological models have been written as differential or integral equations for the fractions in the disease classes, but sometimes models are formulated for the numbers of people in the classes. Connections between these two formulations are discussed extensively in Hethcote and Van Ark (1987). If the models here were formulated in terms of the number of people in the classes and then each equation divided by the constant total populations size N, then the nonlinear incidence rate terms would be $\beta\, g(IN)S/N$. For g(I) given by (3.5),

$$\frac{\beta\, g(I\,N)S}{N} = \frac{\beta\, N^{p-1}\, I^p S}{1 + \alpha\, N^q\, I^q}$$

so that the form is similar to $\beta\, g(I)S$ but $\beta\, N^{p-1}$ and $\alpha\, N^q$ appear as parameters instead of β and α. Thus the two formulations lead to the same model, but the parameters in g(I) are different.

Acknowledgments.

We thank Mark A. Lewis and Wei–min Liu for help with the numerics, Fred Brauer and Wenzhang Huang for discussions on the quasipolynomial (11.2).

References

Busenberg, S., Cooke, K.L.: The population dynamics of two vertically transmitted infections, *Theor. Pop. Biol.* **33**, 181–198 (1988).

Capasso, V., Serio, G.: A generalization of the Kermack–McKendrick deterministic epidemic model, *Math. Biosci.* **42**, 41–61 (1978).

Hale, J.K.: *Ordinary differential equations.* New York: Wiley–Interscience 1969.

Hao, D–Y., Brauer, F.: Analysis of a characteristic equation, *J. Integral Equations and Applications*, 1990. To appear.

Hethcote, H.W.: An immunization model for a heterogeneous population, *Theor. Pop. Biol.* **14**, 338–349 (1978).

Hethcote, H.W., Levin, S.A.: Periodicity in epidemiological models. In: Gross, L., Hallam, T.G., Levin, S.A. (eds.) *Applied Mathematical Ecology.* Berlin, Heidelberg, New York: Springer, 193–211 (1989).

Hethcote, H.W., Lewis, M.A., van den Driessche, P.: An epidemiological model with a delay and a nonlinear incidence rate, *J. Math. Biol.* **27**, 49–64 (1989).

Hethcote, H.W., Stech, H.W., van den Driessche, P.: Nonlinear oscillations in epidemic models, *SIAM J. Appl. Math.* **40**, 1–9 (1981a).

Hethcote, H.W., Stech, H.W., van den Driessche, P.: Stability analysis for models of diseases without immunity, *J. Math. Biol.* **13**, 185–198 (1981b).

Hethcote, H.W., Stech, H.W., van den Driessche, P.: Periodicity and stability in epidemic models: A survey. In: Busenberg, S.N., Cooke, K.L. (eds.) *Differential Equations and Applications in Ecology, Epidemics and Population Problems*, pp. 65–82. New York: Academic Press 1981c.

Hethcote, H.W., Tudor, D.W.: Integral equation models for endemic infectious diseases, *J. Math. Biol.* **9**, 37–47 (1980).

Hethcote, H.W., Van Ark, J.W.: Epidemiological models for heterogeneous populations: proportionate mixing, parameter estimation and immunization programs, *Math. Biosci.*, **84**, 85–118 (1987).

Holling, C.S.: Some characteristics of simple types of predation and parasitism, *Can. Ent.* **91**, 385–395 (1959).

Liu, W.M., Hethcote, H.W., Levin, S.A.: Dynamical behavior of epidemiological models with nonlinear incidence rates, *J. Math. Biol.* **25**, 359–380 (1987).

Liu, W.M., Levin, S.A., Iwasa, Y.: Influence of nonlinear incidence rates upon the behavior of SIRS epidemiological models, *J. Math. Biol.* **23**, 187–204 (1986).

Miller, R.K., Michel, A.N.: *Ordinary Differential Equations.* New York: Academic Press 1982.

van den Driessche, P.: A cyclic epidemic model with temporary immunity and vital dynamics. In: Freedman, H.I., Strobeck, C. (eds.) *Population Biology*, Springer–Verlag Lecture Notes in Biomathematics **52**, 433–440 (1983).

p	q = p		q = p − 1	
< 1	all σ	1	$\sigma \leq \alpha$	0
			$\sigma > \alpha$	1
= 1	$\sigma \leq 1$	0	$\sigma \leq 1 + \alpha$	0
	$\sigma > 1$	1	$\sigma > 1 + \alpha$	1
> 1	$\sigma < \sigma^*$	0		
	$\sigma = \sigma^*$	1		
	$\sigma > \sigma^*$	2		

Table 1

Number of nontrivial equilibria $\in \{0,1,2\}$ with $g(I) = I^p/(1+\alpha I^q)$ for the two cases $q = p$ and $q = p - 1$ showing dependence on σ.

p	q = p		q = p − 1	
< 1	unstable		$\sigma < \alpha$ $\sigma > \alpha$	GAS unstable
= 1	$\sigma \leq 1$ $\sigma > 1$	GAS unstable	$\sigma \leq 1 + \alpha$ $\sigma > 1 + \alpha$	GAS unstable
> 1	LAS GAS for $\sigma < \sigma_1$			

Table 2

Stability of the disease free equilibrium with $g(I) = I^p/(1+\alpha I^q)$
for the two cases $q = p$ and $q = p - 1$ showing
dependence on σ.

Figure Captions

Figure 1. Curves in the $p\alpha$ plane are shown for $p = p_1$ where the Hopf–bifurcation surface $\sigma = \sigma^{**}$ originates on the saddle–node bifurcation surface $\sigma = \sigma^{*}$ and for $p = p_2$ where the sign of the stability quantity A first switches from positive to negative. Cases $q = p$ and $q = p - 1$ are shown when g(I) is given by (3.5). The parameter values are $\epsilon = 1$, $\gamma = 0.0133$, $\delta = 0.0033$ and $\mu = 0.00004$.

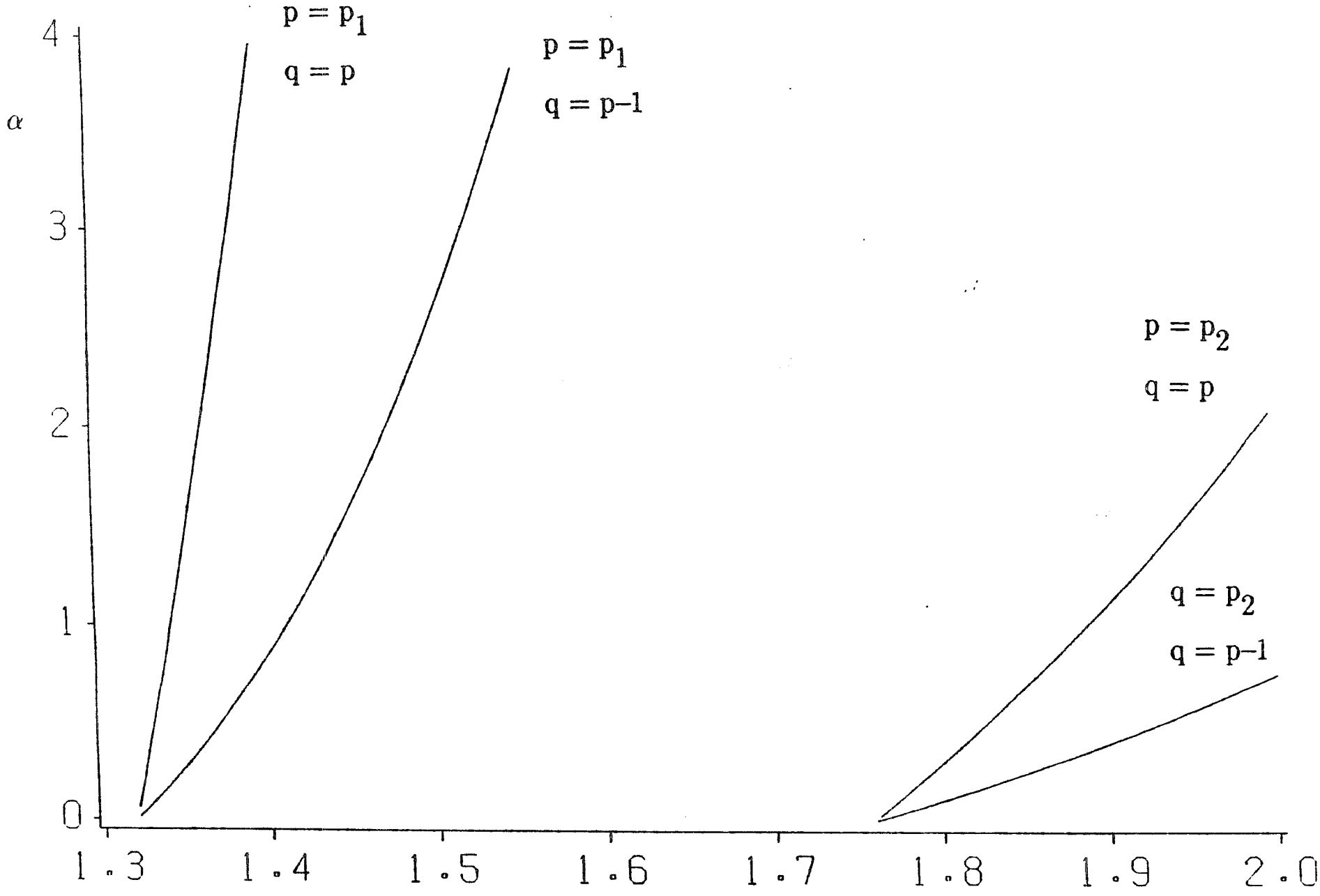

FIGURE 1